This is a peer-reviewed, accepted author's manuscript of the following conference paper: Wei, Y., & Tezdogan, T. (2022). *A fluid-structure interaction model on the hydroelastic analysis of a container ship using PRECICE.* Paper presented at 41st International Conference on Ocean, Offshore and Arctic Engineering, Hamburg, Germany

OMAE2022-78131

A FLUID-STRCUTURE INTERACTION MODEL ON THE HYDROELASTIC ANALYSIS OF A CONTAINER SHIP USING PRECICE

Yujia Wei, Tahsin Tezdogan

Department of Naval Architecture, Ocean and Marine Engineering, University of Strathclyde,

100 Montrose Street, Glasgow G4 0LZ

ABSTRACT

Commercial vessels have recently shown a common trend in increasing their sizes to meet the growing demand for transportation and operations. This trend may however result in more flexible or 'softer' hulls. The flexible hull structure reduces the ship natural frequency close to the wave encounter frequency, increasing the probability of resonance or high-frequency vibrations. Meanwhile, the resulting structural deformations from flexible hull could significantly affect the flow field and the hydrodynamic loads cannot be estimated accurately. Hence, it is important to treat a flexible hull and its surrounding flow field as an interacting system to predict a ship's dynamic behaviour based on the hydroelastic theory. In this study, a novel fluid-structure interactions coupling scheme using the "preCICE" library to communicate with the fluid solver "OpenFOAM" and structure solver "calculiX" was first proposed to study the hydroelastic behavior of a container ship with a forward speed in regular waves. With the advantage of this numerical model, the flexible behaviour of this ship, such as its vertical bending displacement and corresponding bending moment can be quantified, and the "springing" and "whipping" responses can be calculated. It is believed that the present FSI model will exhibit more advantages over the traditional rigid-body methods currently used in the ship seakeeping field.

Keywords: Ship hydrolasticity, Fluid-structure Interaction, slamming, ship motion, CFD, FEA, vertical bending moment

1. INTRODUCTION

For the structural integrity and safety concerns of the large vessels, such as container ships operating in waves, the hydroelastic response of these ships is of particular importance since the vibration induced loads are superposed to the wave-induced load that may enlarge the structure responses [2]. In such cases, the deformation of the structure may significantly violate the surrounding flow fields, forming a fully coupled system. The original rigid ship assumption may lead to inaccurate prediction of hydrodynamic loadings as well as the ship motions. Therefore, a quantitative Fluid Structure Interaction (FSI) method for predicting the accurate hydrodynamic forces and subsequent hydroelastic responses of a container ship under wave excitations is required.

The pioneering work of Bishop, R. E. D. et al. developed a linear Fluid Structure Interaction model on the basis of 2D potential flow theory and linear beam model [1]. Their calculation in the frequency domain was faster and valuable in providing insight in the early design stage of a vessel [13]. Great deal of progress has been made since then in the development and application of the frequency domain of 2-D and 3-D hydroelasticity analyses on ship structures [3, 4, 14, 15, 16, 25].

However, some physical phenomena such as wave breaking, slamming and viscous effects cannot be included in potential flow method. To account for these effects, a fully nonlinear CFD method, which solves the Navier-stokes equations is commonly used as an alternative to potential flow theory. The hydroelastic behavior of a flexible ship with surrounding fluids using the above nonlinear method can be modelled by coupling it with a structural Finite Element Analysis (FEA) method [12]. This CFD-FEA coupling forms a partitioned approach of FSI, which reduces the efforts to adapt the original computational models [23] and preserves both the advanced features of the CFD and FEA solvers [22] against the monolithic approach [26].

The implicit coupled method between CFD and FEA has been employed to simulate the flexible ship responses in

nonlinear seaways and to predict the corresponding wave-induced motions and loads [17, 18]. Paik, K. J. et al. [23] designed a structure model using rigid ship segments intersected with small elastic beams using ABAQUS and solved the fluid flow by CFDShip-lowa. Two software packages were strongly coupled using data communications gluing method. Ma, S. et al. [8] investigated the local strength behaviors of a composite catamaran hull by discretizing the whole ship geometry in the ANSYS structure solver. The surrounding ship flow field was resolved by a CFX solver. A two-way coupling framework was established between the structure and fluid solver based on ANSYS workbench. The local fragile region was highlighted at the sandwich plating between hull layers by using this coupling framework. EI Moctar, O. et al. [11] proposed an implicit interaction method to assess wave-induced structural loads of three slender containerships in regular and irregular waves using a ship-beam segments model. The computational model was built with an in-house structure solver and linked to RANSE solver COMET and interFoam [11]. Lakshmynarayanana, P. A. et al. [13], Takami, T. et al. [27] and Jiao, J. et al. [6] investigated the symmetric motions and loads on a S175 containership undergoing severe waves based on the commercial co-simulation packages (Star-ccm+ & Abaqus). Their results, including ship RAOs and VBM, were validated well with the experiments. In addition, the ship springing and whipping responses induced by high frequencies were captured accurately. Moreover, Jiao, J et al. [5] further investigated on the slamming pressure and green water on deck of the S175 container ship under severe wave conditions.

As a brief review of the above indicates, the numerical studies on the ship hydroelasticity have mostly relied on the commercial coupling software or in-house codes, which a license is required, or it is hard to reproducible. To extend the possibilities and test the performance of existing open-source FSI packages, in the present paper, a peer-to-peer coupling library "preCICE" which coupled OpenFOAM and CalculiX is first used to investigate the hydroelastic motion and loads of a containership (S175) in regular waves. The rest of this paper is organized as follow: in Section 2, the numerical setting ups and the methodology used in the present study are discussed. In Section 3, the numerical results for the study on the dynamic motion of the flexible S175 ship in waves are presented and compared with another commercial FSI package as well as the experimental results. Both global ship motions and hydroelastic behavior are included. The conclusions are drawn in the final section.

2. NUMERICAL METHODS

In the present Fluid Structure Interaction study, we used a partitioned coupling scheme to separate the solution domain into a fluid domain and structure domain and solving them iteratively. The detailed numerical methods of both fluid and solver solvers are described in the following sub-sections.

2.1 Fluid dynamics

2.1.1 Governing equations

The mass continuity and momentum equations for a transient, incompressible, and viscous fluid can be written as

$$\nabla \cdot U = 0 \tag{1}$$

$$\frac{\partial \rho U}{\partial t} + \nabla \cdot (\rho UU) - \nabla \cdot \tau = -\nabla P_d + \rho g + F \tag{2}$$

where U refers to the velocity of flow field, ρ is the mixed density of water and air, g is the gravity acceleration, P_d refers to the dynamic pressure, τ is the dynamic viscosity, F is the surface tension.

The VOF technique was adopted to simulate the free surface using an additional transport equation to solve for the volume fraction *a.* In multiphase flows, the volume fraction is assigned a value of 0 when the cells are filled with air, and when it is 1 the cell is filled with water.

2.1.2 Computational domain and mesh generation

The finite volume mesh was generated by the mesh generation tool "SnappyHexMesh" based on a cell splitting and body fitting technique [9]. The numerical domain used to simulate ship motions in waves extends in three directions, i.e., $-1.5L < x < 2.0L$, $-1.0L < y < 1.0L$ and $-1.5L < z < 1.0L$, where L refers to the ship length between perpendiculars (4.375*m, see Table 1*) [7]. The grids density at the free surface zone was progressively refined several times to fulfil the guideline from ITTC (2017) [21]. According to these recommendations, a minimum of 120 cells per wavelength and 12 cells per wave height were used on the free surface in this study as shown in Figure 1 [7]. The choice of the K-omega SST turbulence model further required a more refined mesh at the area immediately around the ship hull, primarily maintained the adjacent wall layer thickness coordinate $y+$ close to 30 associated with the higher Reynolds number flow [24].

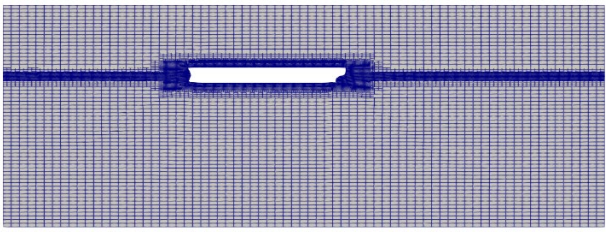

FIGURE 1: THE COMPUTATIONAL DOMAIN MESH LAYOUT.

2.1.3 Boundary conditions

The boundary conditions of the present CFD model were defined as follows. At the left boundary inlet, the velocity was prescribed as the incident wave and current, while the pressure was set as zero gradient. At the right boundary outlet, the current velocity outlet was applied to preserve the conservative of flux inside the computational domain. The boundary condition of the domain top part was set as atmosphere. The domain bottom boundary was set as symmetry plane which represented a deep-water condition as well as the lateral sides. The moving wall boundary condition with zero pressure gradient was defined on the surface of the ship hull.

2.1.4 Wave generation and absorption

The wave generation library "waves2Foam" was integrated to the OpenFOAM solver "interFoam" to generate and absorb waves in the computational domain [9, 10]. The second Stokes waves theory was used to generate the regular waves throughout all the cases. The forward speed of ship was modelled by combining a uniform-velocity current at the wave boundary inlet. The service speed of the ship in full scale was 20 knots, which was modelled by applying a reversed uniform flow speed of 1.32m/s at domain boundary inlet. The wave absorption relied on the relaxation zone technique using Eqn. 3 and Eqn. 4 [10].

$$a_R(\chi_R) = 1 - \frac{\exp(\chi_R^{3.5}) - 1}{\exp(1) - 1} \tag{3}$$

$$\phi_R = \omega_R \phi_R^{computed} + (1 - \omega_R)\, \phi_R^{target} \tag{4}$$

where ϕ_R refers to either the velocity or volume fraction of water a. The definition of χ_R is that the weighting function a_R is always 1 at the interface between the non-relaxed computational domain and the relaxation zones, and χ_R is a value between 0 and 1.

2.2 Solid dynamics

2.2.1 Governing equations of Timoshenko beam

In the present study, the equations for transverse vibration of the uniform Timoshenko beam with a constant cross section can be expressed as given below: [19, 20]

Force equation

$$\mathrm{m(x)}\frac{\partial^2 \mathrm{y(x,t)}}{\partial \mathrm{t}^2} - \frac{\partial \mathrm{Q(x,t)}}{\partial \mathrm{x}} = f_3(x,t) \tag{5}$$

Moment equation

$$-\frac{\partial \mathrm{M(x,t)}}{\partial \mathrm{x}} + \mathrm{Q(x,t)} - I\rho\frac{\partial^2 \Theta(\mathrm{x,t})}{\partial \mathrm{t}^2} = 0 \tag{6}$$

where $\mathrm{m(x)}$ is body mass per unit length, $\mathrm{y(x,t)}$ is displacement amplitude, $\mathrm{Q(x,t)}$ is shear force, calculated by $\mathrm{Q(x,t)} = GA\gamma(\mathrm{x,t})$, G is shear modulus, A is cross section, $\mathrm{M(x,t)}$ is bending moment, has an equation of $\mathrm{M(x,t)} = EI\,\partial\Theta(\mathrm{x,t})/\,\partial\mathrm{x}$, where EI is the flexural stiffness, $f_3(x,t)$ is time dependent vertical hydrodynamic force per unit length.

2.2.2 Ship description

The benchmark S175 type of containership with a scale ratio of 1:40 was used in this study. The body plan of full-scale ship is shown in Figure 2. The main dimensions of the ship in the model- and full-scales are shown in Table 1.

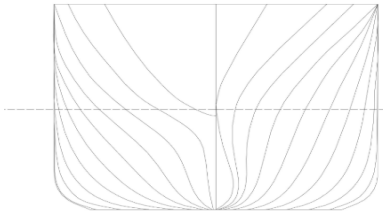

FIGURE 2: BODY PLAN OF THE S175 HULL [6].

TABLE 1: MAIN PROPERTIES OF THE S175 CONTAINERSHIP.

Ship Geometry description	Full scale	Model
Scale	1:1	1:40
Length between perpendiculars (L)	175 *m*	4.375 *m*
Breath (B)	25.4 *m*	0.635 *m*
Draft (T)	19.5 *m*	0.488 *m*
Displacement (A)	23,711 t	370 kg
Block coefficient (C_b)	0.562	0.562
Longitudinal center of gravity (LCG) from after perpendicular	84.980 *m*	2.125 *m*
Vertical center of gravity (KG) from base line	8.5 *m*	0.213 *m*
Transverse radius of gyration	9.652 *m*	0.241 *m*
Longitudinal radius of gyrations	42.073 *m*	1.052 *m*

2.2.3 Structural model

In this study, a ship-beam segment model based on a beam-shell coupling approach which comprises a massless ship surface shell (including main deck) and a backbone beam, was built in the open-source FEA software CalculiX [30]. The hull surface was lengthwise cut for 20 sections as shown in Figure 4, and then discretized using 3-node triangular shell elements (S3), which in total 50,247 elements were used (mesh in Figure 3). The elements at hull surfaces were rigidly connected with the nodes at backbone beam, which allowed the forces and moments at the shell surfaces transferring to the beam nodes.

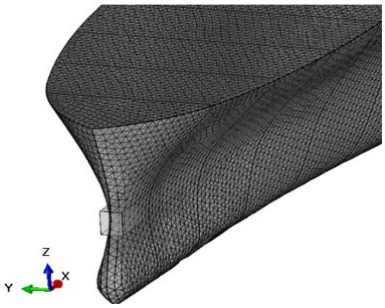

FIGURE 3: SHIP HULL DISCRETIZATION.

The backbone beam based on Timoshenko beam theory, whose governing equations are shown in Section 2.2.1, was modelled using B32R beam elements. It is worth noting that the B32R beam element was the preferred beam element of selections. It performs well for bending behavior and avoids the shear locking and volumetric locking against other beam elements supported by CalculiX [30]. The backbone beam was positioned at a height of vertical center of gravity of ship model. The ship mass modelled as distributed point mass, which was placed on the beam elements as shown in Figure 4 and Figure 5. The material property of beam was defined as steel, i.e., elastic stiffness$\mathrm{E} = 210Gpa$ and Poisson ratio $v = 0.3$.

The cross section of backbone beam was determined by calibrating the natural frequency of the beam to match with the 2-node dry natural frequency of ship hull. The detailed estimation of both beam and ship natural frequencies is presented in Section 2.2.4. The FE model was constrained for the y-axis translation and rotation by imposing constraints on the beam and shell nodes. Moreover, the beam center node was restrained in the direction of x-axis to avoid ship drift by the waves.

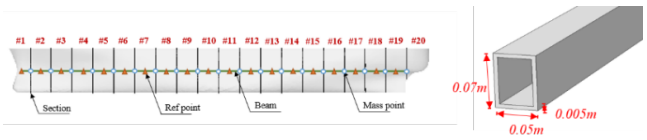

FIGURE 4: SHIP BEAM SEGMENT MODEL SETTINGS.

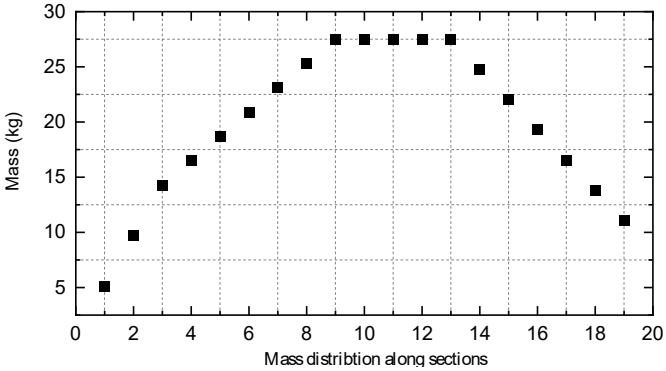

FIGURE 5: THE MASS DISTRIBUTION AT EACH SHIP SECTION ALONG THE LONGITUDINAL AXIS.

2.2.4 Dry frequency analysis

The natural frequencies of the dry ship were estimated in vacuum, which assumed the free-free beam structure stayed in the absence of any external actions or internal damping. To avoid asymmetric effects (i.e., torsion or horizontal bending), the y-symmetry boundary conditions were applied for the FE model. The first three modes were calculated as listed in Table 2 and its deformation were shown in Figure 6.

When bending or torsional loads are not applied on the beam symmetry line, the beam may produce warping or nonuniform out of plane displacement. Although the warping effects due to the pure bending are small, a box-shaped beam section is assigned to the beam profile since this closed-type cross section is free from warping effects compared with open sections. The beam thickness and section dimensions were determined by matching the second node natural frequencies of the ship-beam model with the full-scale ship. After calibration, the beam profile with a cross-section of $0.07m$ * $0.05m$ and thickness $0.005m$, as shown in Figure 4, was used through all later cases in this study.

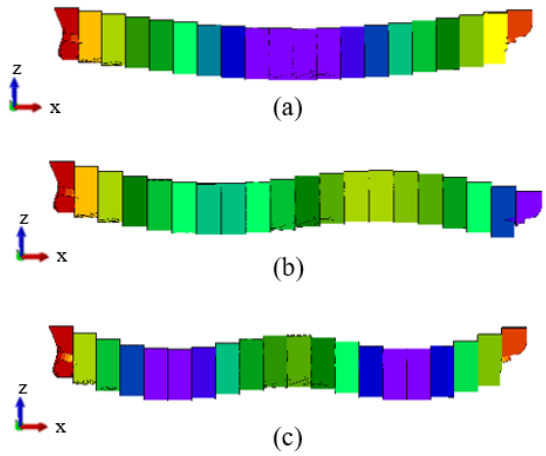

FIGURE 6: DRY SHIP NATURAL FREQUENCY VISULIZATION.

2.2.5 Wet frequency analysis

An additional natural frequency estimation of the wet mode of hull was modelled based on a continuum-based fluid modelling approach using a commercial finite element software Abaqus/CAE 2020. In this type of application, the added mass effect was an important parameter to consider by modeling the surrounding infinite of water. The wet surface of ship hull was encapsulated in a fluid zone, and a pair of fluid-solid coupling surfaces were generated between the free surface and ship wet surface.

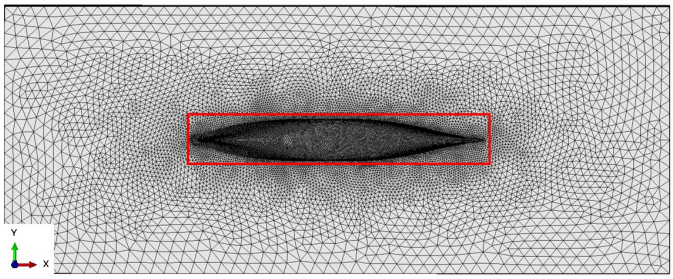

FIGURE 7: ACOUSTIC FLUID DOMAIN.

The acoustic medium, modelled by S4 acoustic element assigning with water density $1{,}025\text{kg}/m^3$ was used to simulate the sea water condition. Figure 7 shows the dimension of the acoustic computational tank used in this study. It has 9.0 meter in length and 6.0 meter in width, and it is discretized in 46,589 number of elements. The mesh region adjacent to the ship was kept a consistent grid density to the ship surface mesh (red square), and the mesh density was reduced outwards to the far field. Two boundaries were applied; a non-reflection boundary condition via a surface impedance for the outer surfaces of the domain to avoid the water reflection and a kinematic coupling boundary for the ship wet surface to ensure the displacement field in the structure was coupled with the fluid pressure field. The first three modal shapes of ship in wet frequency analysis were shown in figure 8.

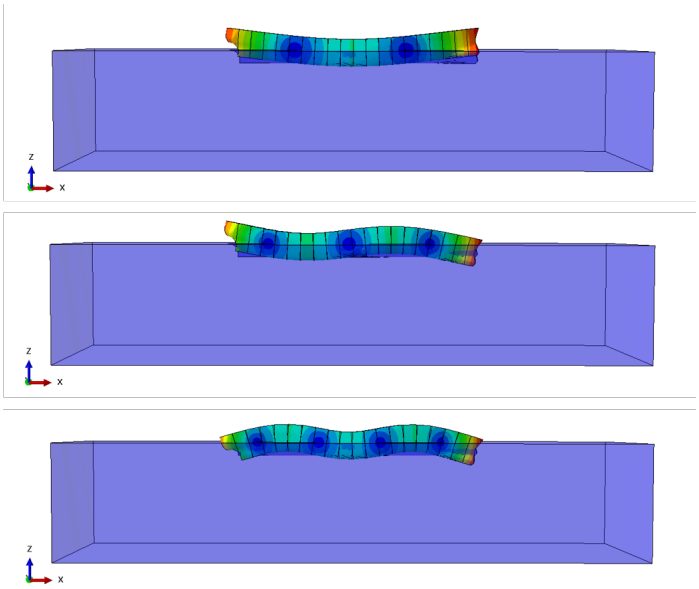

FIGURE 8: WET SHIP NATURAL FREQUENCY VISULIZATION.

Both dry and wet natural frequency models were solved using the SPOOLES solver. The results were shown in Table 2 and compared with the experimental results listed in Error* columns. As expected, wet natural frequencies of the ship were significantly lower than dry natural frequencies due to the consideration of hydrodynamic added mass.

TABLE 2: CALIBRATED BEAM NATURAL FREQUENCY PROPERTIES AND ERRORS.

Order	Mode	Dry condition (Hz)	Error* (%)	Wet condition (Hz)	Error* (%)
1st	2-node	9.54	5.9%	8.17	7.6%
2nd	3-node	25.02	4.6%	21.28	6.6%
3rd	4-node	48.04	3.4%	40.70	5.9%

2.3 Fluid structure interaction model

A two-way Fluid Structure Interaction framework is proposed in this study as a first time to study the hydroelastic response of a containership in regular waves via an elaborate coupling library “preCICE” [28].

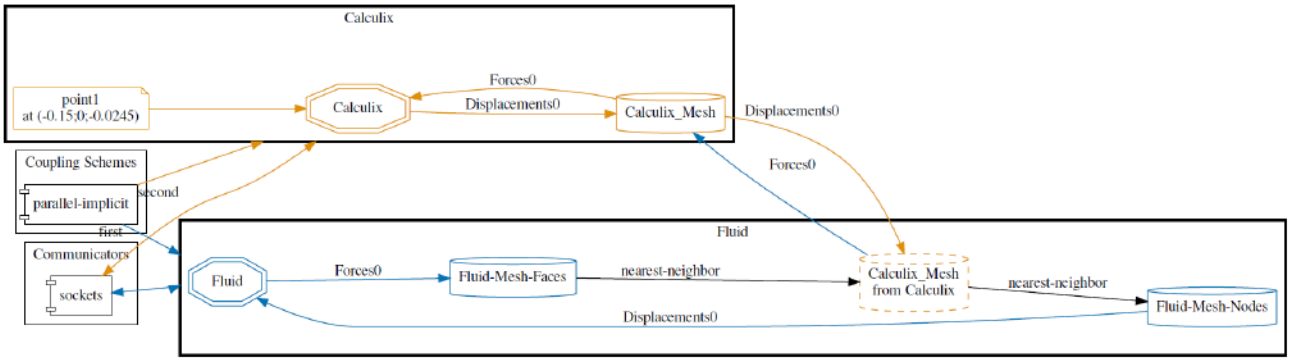

FIGURE 9□ FLUID STRUCTURE INTERACTION WORK FLOW.

The main configuration is shown in Figure 9. A parallel implicit algorithm was applied to couple the fluid solver "OpenFoam" and solid solver "CalculiX" using a peer-to-peer approach as shown in Figure 9. Two official adapters, OpenFOAM adapter [29] and CalculiX adapter [31] are plug in for data communications. An improved IQN-ILS method was employed to stabilize and accelerate the coupling iterations. To map the data between a pair of non-matched grids of fluid and solid meshes, the nearest neighbor mapping scheme was used which is a first order method and it directly mapped the data through the closest nodes. As shown in Figure 10, the fluid mesh density was designed finer than the solid mesh, in order to calculate the fluid force more precisely and eliminate the numerical instability at the initial conditions. The consistent mapping was applied for the transformation of displacements, while a conservative mapping was used for forces for energy balance.

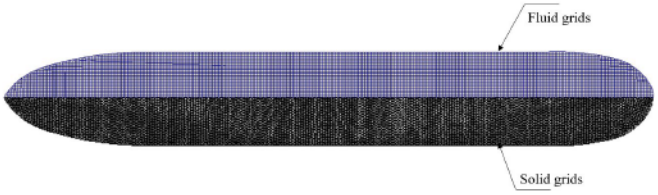

FIGURE 10: WET SURFACES BETWEEN FLUID AND SOLID.

3. RESULTS

In this section, the global ship motions and corresponding hydroelastic behaviors of the S175 containership at wave length (λ/L=1.2) with a forward speed of $F_n = 0.2$ are analyzed. The case was run parallel using multi-nodes (80 cores) on HPC, the averaging time step was set as 0.002s. The simulation was run up to 5 complete wave periods for attaining stable results and the required physical time was about 300 hours.

The time series of flexible ship heave motions were monitored on the real-time displacement of the beam node close to the ship gravity center, as shown in Figure 11. The flexible ship responses of current ship-wave matching resonance case showed a slightly lower value at the peak by about 15% when compared to the rigid body cases.

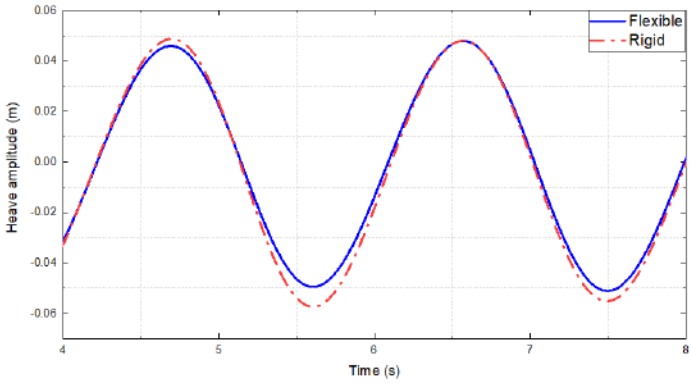

FIGURE 11: CALCULATED HEAVE MOTION AT λ /L=1.2.

In addition, the corresponding pitch motions of both flexible and rigid body cases are presented in Figure 12. Both heave and pitch results are in regular and sinusoidal shapes, which indicate the suitability of the present solvers on seakeeping.

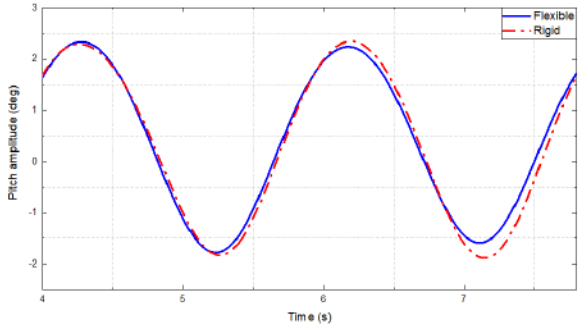

FIGURE 12: CALCULATED PITCH MOTION AT λ/L=1.2.

It is worth mentioning that the structure solver CalculiX does not have an internal rotational degrees of freedom [30]. Therefore, the pitch angle was calculated using the relative difference ratio between two adjacent nodes of vertical and horizontal distances based on a linear approximation equation as given in Equation 7.

$$\theta = \arctan\left(\frac{z_c - z_{c+1}}{x_c - x_{c+1}}\right) * \frac{180}{\pi} \quad (7)$$

where, θ is the pitch angle in degree, subscript c points to the beam node at ship gravity center, and $c+1$ means the corresponding adjacent node sequence. The raw pitch data is given in radians, therefore, a factor of 180/π is multiplied to convert it into degrees.

The RAOs of ship motions were estimated by using the motion data and wave amplitudes from the last two stable wave periods. These RAO results were then compared with the co-simulation results from Jiao et al. [5] and the experimental data from Chen et al. [32] as shown in Figure 13. The heave (z) and pitch (θ) motions are non-dimensionalized by z/ξ and $\theta/k\xi$, where ξ is estimated wave amplitude, respectively. From Figure 13, the present heave RAOs are found to be 16.3% lower than the co-simulation results and 18.0% lower than the experimental data. The deficiencies may be caused by the inconsistent selections of coupling methods, structure solver demonstrations, as well as the time step resolutions between the existing solvers and comparatives. A comprehensive convergence test including mesh densities and time step sizes will be studied in the future. Moreover, the calculated pitch RAOs show a good agreement with the experimental data [32].

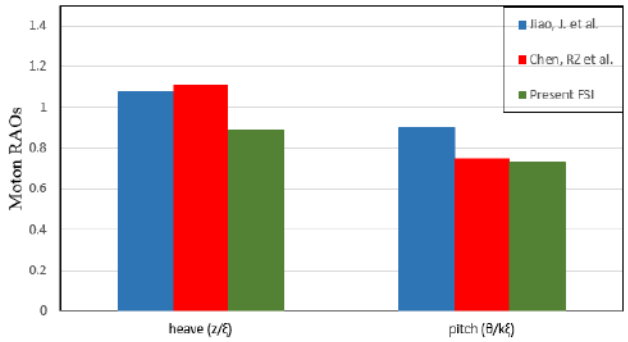

FIGURE 13: SHIP RAOs AT λ/L=1.2 COMPARED WITH LITERATURES.

The peaks of vertical bending moment (VBM) were extracted at the ship mid-section and compared with the results from co-simulation [5] as shown in dashed lines in Figure 14. In addition, the first harmonic of wave bending moment was extracted from the total VBM component by using bandwidth pass filtering, and its peaks are shown in solid lines in Figure 14. Overall, the magnitudes of these peak values from the present FSI model were generally lower than the results from the co-simulation.

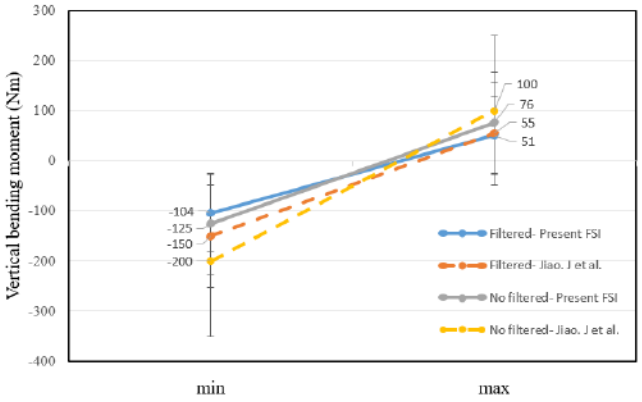

FIGURE 14: COMPARISONS OF VBM PEAK VALUES.

The hogging and sagging peak values at each ship sections in the case of λ/L=1.2 were further compared with the co-simulation results [5], which are presented in Figure 15. The VBM (M) is non-dimensionalized by $M/\rho g L^2 B\xi$. As can be seen in Figure 15, the results indicate similar trends of the hogging and sagging curves between the present FSI model and the co-simulation model, except when the peak values are lower in general as noticed above. From Figure 15, both models successfully captured the asymmetry behavior of hogging and sagging moments along the ship sections. The peak value of hogging VBM occurred at ship 10th section, which was evidenced from both the present FSI and co-simulation model. However, the position of the trough peak values of sagging VBM from co-simulation appears at 9th section compared with 10th section from the present model.

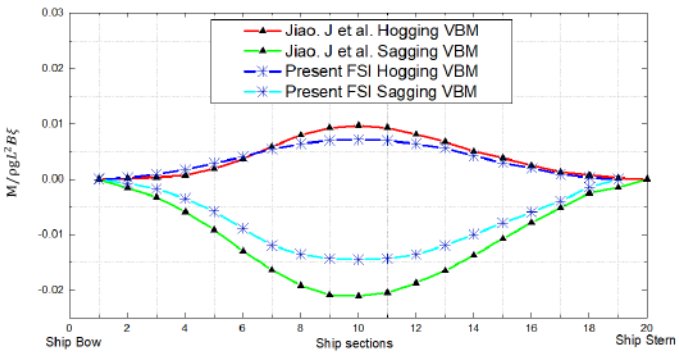

FIGURE 15 COMPARISONS OF VBM ALONG SHIP SECTIONS.

4. CONCLUSION

In this study the seakeeping and hydroelastic behavior of a flexible S175 containership has been modelled through an open-source coupling FSI framework. The resonance case of the ship in question in head waves was investigated and validated by comparing the ship motions and VBM results with the experimental measurements [32] and co-simulation FSI packages results [5]. The vertical motions predicted by the present FSI model generally agreed well with experimental results, except the heave RAOs. The peak values of ship total VBM and hogging/sagging moments showed similar trends with the co-simulation results. In general, this study showed the present FSI codes capacity to predict the hydroelastic behavior of a containership in heading waves. Future pieces of work will focus on more extensive studies on different wave conditions as well as ship forward speeds and on the extreme wave effects on flexible ship responses by performing the models in short-crested irregular waves.

5. ACKNOWLEDGEMENTS

The authors would like to acknowledge the numerical results were obtained using the ARCHIE-WeSt High Performance Computer (www.archie-west.ac.uk) based at the University of Strathclyde.

REFERENCES

[1] Bishop, R. E. D., Bishop, R. E., & Price, W. G. (1979). *Hydroelasticity of ships*. Cambridge University Press.

[2] Hirdaris, S., & Temarel, P. (2009). Hydroelasticity of ships: recent advances and future trends. *Proceedings of the Institution of Mechanical Engineers, Part M: Journal of Engineering for the Maritime Environment*, *223*(3), 305-330.

[3] Faltinsen, O. M. (1997). The effect of hydroelasticity on ship slamming. *Philosophical Transactions of the Royal Society of London. Series A: Mathematical, Physical and Engineering Sciences*, *355*(1724), 575-591.

[4] Senjanović, I., Malenica, Š., & Tomašević, S. (2009). Hydroelasticity of large container ships. *Marine Structures*, *22*(2), 287-314.

[5] Jiao, J., Huang, S., Tezdogan, T., Terziev, M., & Soares, C. G. (2021). Slamming and green water loads on a ship sailing in regular waves predicted by a coupled CFD–FEA approach. *Ocean Engineering, 241,* 110107.

[6] Jiao, J., Huang, S., & Soares, C. G. (2021). Viscous fluid–flexible structure interaction analysis on ship springing and whipping responses in regular waves. Journal of Fluids and Structures, 106, 103354

[7] Tezdogan, T., Demirel, Y. K., Kellett, P., Khorasanchi, M., Incecik, A., & Turan, O. (2015). Full-scale unsteady RANS CFD simulations of ship behaviour and performance in head seas due to slow steaming. *Ocean Engineering*, *97*, 186-206.

[8] Ma, S., & Mahfuz, H. (2012). Finite element simulation of composite ship structures with fluid structure interaction. *Ocean Engineering,* 52, 52–59. https://doi.org/10.1016/j.oceaneng.2012.06.010

[9] Jasak, H., Jemcov, A., & Tukovic, Z. (2007, September). OpenFOAM: A C++ library for complex physics simulations. In International workshop on coupled methods in numerical dynamics (Vol. 1000, pp. 1-20). IUC Dubrovnik Croatia.

[10] Jacobsen, N. G., et al. (2012). "A wave generation toolbox for the open-source CFD library: OpenFoam®." *International Journal for Numerical Methods in Fluids 70(9)*: 1073-1088.

[11] EI Moctar, O., et al. (2017). "Nonlinear computational methods for hydroelastic effects of ships in extreme seas." *Ocean Engineering 130*: 659-673.

[12] Hirdaris, S. E., et al. (2014). "Loads for use in the design of ships and offshore structures." *Ocean Engineering 78*: 131-174.

[13] Lakshmynarayanana, P. A. and P. Temarel (2020). "Application of a two-way partitioned method for predicting the wave-induced loads of a flexible containership." Applied Ocean Research 96.

[14] Bishop, R. E. D., Price, W. G., & Wu, Y. (1986). A general linear hydroelasticity theory of floating structures moving in a seaway. *Philosophical Transactions of the Royal Society of London. Series A, Mathematical and Physical Sciences*, 316(1538), 375-426.

[15] Bishop, R. E. D., Price, W. G., & Temarel, P. (1980). Hydrodynamic coefficients of some swaying and rolling cylinders of arbitrary shape. *International Shipbuilding Progress*, *27*(307), 54-65.

[16] Senjanović, I., Malenica, Š., & Tomašević, S. (2008). Investigation of ship hydroelasticity. *Ocean Engineering*, *35*(5–6), 523–535.

[17] Seng, S., Jensen, J. J., & Malenica, Š. (2014). Global hydroelastic model for springing and whipping based on a free-surface CFD code (OpenFOAM). *International Journal of Naval Architecture and Ocean Engineering*, *6*(4), 1024–1040. https://doi.org/10.2478/IJNAOE-2013-0229

[18] Lakshmynarayanana, P. A. K., & Hirdaris, S. (2020). Comparison of nonlinear one- and two-way FFSI methods for the prediction of the symmetric response of a containership in waves. *Ocean Engineering*, 203(February), 107179. https://doi.org/10.1016/j.oceaneng.2020.107179

[19] Faltinsen, O. (2006). SLAMMING, WHIPPING, AND SPRINGING. In Hydrodynamics of High-Speed Marine Vehicles (pp. 286-341). Cambridge: Cambridge University Press.
https://doi.org/10.1017/CBO9780511546068.009

[20] Majkut, L. (2009). Free and forced vibrations of timoshenko beams described by single difference equation. *Journal of Theoretical and Applied Mechanics*, *47*(1), 193–210.

[21] International Towing Tank Conference (ITTC), 2014. Practical guidelines for ship CFD applications. In: Proceedings of the 28th ITTC.

[22] Luo, Y., Xiao, Q., Shi, G., Wen, L., Chen, D., & Pan, G. (2020). A fluid–structure interaction solver for the study on a passively deformed fish fin with non-uniformly distributed stiffness. *Journal of Fluids and Structures*, 92, 102778. https://doi.org/10.1016/j.jfluidstructs.2019.102778

[23] Paik, K. J., Carrica, P. M., Lee, D., & Maki, K. (2009). Strongly coupled fluid-structure interaction method for structural loads on surface ships. *Ocean Engineering*, *36*(17–18),1346–1357.
https://doi.org/10.1016/j.oceaneng.2009.08.018

[24] Menter, F. R. (1992). Improved two-equation k-omega turbulence models for aerodynamic flows. Nasa Sti/recon Technical Report N, 93, 22809.

[25] Kim, J. H., & Kim, Y. (2014). Numerical analysis on springing and whipping using fully coupled FSI models. *Ocean Engineering*, *91*, 28-50.

[26] Benra, F. K., Dohmen, H. J., Pei, J., Schuster, S., & Wan, B. (2011). A comparison of one-way and two-way coupling methods for numerical analysis of fluid-structure interactions. *Journal of applied mathematics*, *2011*.

[27] Takami, T., Matsui, S., Oka, M., & Iijima, K. (2018). A numerical simulation method for predicting global and local hydroelastic response of a ship based on CFD and FEA coupling. *Marine Structures*, *59*(August 2017), 368–386. https://doi.org/10.1016/j.marstruc.2018.02.009

[28] Bungartz, H. J., Lindner, F., Gatzhammer, B., Mehl, M., Scheufele, K., Shukaev, A., & Uekermann, B. (2016). preCICE–a fully parallel library for multi-physics surface coupling. *Computers & Fluids*, 141, 250-258.

[29] Chourdakis, G. (2017). A general OpenFOAM adapter for the coupling library preCICE.

[30] Dhondt, G. (2004). The finite element method for three-dimensional thermomechanical applications. John Wiley & Sons.

[31] Uekermann, B., Bungartz, H. J., Yau, L. C., Chourdakis, G., & Rusch, A. (2017, October). Official preCICE adapters for standard open-source solvers. In Proceedings of the 7th GACM Colloquium on Computational Mechanics for Young Scientists from Academia.

[32] Chen, R. Z., Du, S. X., Wu, Y. S., Lin, J. R., Hu, J. J., & Yue, Y. L. (2001). Experiment on extreme wave loads of a flexible ship model. In Practical Design of Ships and Other Floating Structures. Proceedings of the Eighth International Symposium on Practical Design of Ships and Other Floating StructuresPRADS (Practical Design in Shipbuilding) Chinese Academy of Engineering, Chinese Society of Naval Architects and Marine Engineers, Chinese Institute of Navigation (Vol. 2).